

LIGO PROJECT STATUS UPDATE

A. LAZZARINI

California Institute of Technology, LIGO Laboratory, MS 18-34

Pasadena, California 91125, USA

LIGO-P990024-00-E

Over the past year LIGO began its operational phase and made a transition from a construction project to a laboratory. Civil construction of facilities is complete at both observatory sites. All vacuum equipment have been successfully delivered and accepted at both observatories. All beam tubes have been accepted at both observatories. The bakeout of the beam tube at Hanford has been completed and the Livingston system will begin bakeout in June/July 1999. The design of the detector is now complete and detector fabrication is in full swing, with all major procurement contracts in place. Detector installation at both observatories is under way. Data analysis systems and simulation systems are being implemented to support commissioning of the first subsystems.

1 Observatories

Figure 1 LIGO Hanford Observatory



LIGO Hanford Observatory (LHO, **Figure 1**). At Hanford all infrastructure was successfully completed by the end of 1998. Beneficial occupancy began and currently only LIGO Laboratory and scientific collaborators are present at the Observatory. The LIGO Laboratory staff is approximately 50% complete.

LIGO Livingston Observatory (LLO, **Figure 2**). At Livingston all infrastructure was successfully completed by January 1999. The LIGO Laboratory staff is approximately 25% complete.

At both observatories all laboratories have been equipped and are operational. The observatories

have already hosted a number of meetings, including the annual NSF review, LIGO Program Advisory Committee and Scientific Collaboration and GWIC meetings.

Scientific research in support of eventual LIGO operations at the two sites is being conducted on the physical environment (seismic ground motions, ambient electromagnetic field environment, air quality, etc.) and on initial interferometer subsystems (seismic and suspension isolation systems; prestabilized laser system, etc.). During summer 1999 a number of students (graduate and undergraduate) will be participating in this research under the managership of the local scientific staff.

Telecommunications infrastructure has been established at both sites. A LIGO wide area network has been set up which provides LIGO Laboratory with a coast-to-coast communications capability at T1 bandwidth (1.55 Mb/s). LHO relies on an MOU with the US Department of Energy to access DoE's ESnet services by way of a gateway established at Battelle (Pacific Northwest National Laboratory, PNNL). LLO relies on a link by way of gateway services provided by Louisiana State University (LSU) in Baton Rouge, LA.

Figure 2 LIGO Livingston Observatory



orel formulation which does not suffer from the before the beam tube bakeout begins at LLO.

At LLO, preparation for bake out of the beam tubes is under way. Installation of thermocouples is in progress. Insulation and electrical installation work for the bakeout will begin in summer 1999. The bakeout will be completed at LLO by June 2000.

In general, the plan has been that installation activities at LLO will lag LHO by approximately 6 - 9 months because of the sequential nature of many of the construction and installation activities.

The recent major focus at LHO has been baking out of the beam tubes in preparation for operation. The beam tubes have been baked successfully and are presently under

The last of LIGO vacuum equipment was accepted at LLO in January 1999 (**Figure 3**). After the bakeout conducted by the manufacturer as part of acceptance tests, the vacuum equipment system was demonstrated to meet LIGO requirements (**Table 1**). Due to the large apertures in LIGO chambers, the vacuum equipment design was constrained to use visco-elastomer (Viton, fluorel) O-ring material. One nuisance discovered in the bake process for the vacuum chambers is that Viton loses its resilience when baked under pressure to high temperatures (the material becomes stiff). To correct this situation, certain large aperture O-rings will be replaced with a flu-hardening. This replacement can be done in time

Figure 3 LLO vacuum equipment



operation-ready condition, awaiting “first light” from the interferometers. **Figure 4** shows the insulated beam tube during bakeout.

Table 1 LLO VE performance data (torr)

Species (AMU)	Y End	X End	Vertex	Required
2	5.8×10^{-9}	5.2×10^{-9}	3.7×10^{-9}	$<5 \times 10^{-9}$
16	3.3×10^{-11}	4.0×10^{-11}	4.3×10^{-11}	$<2 \times 10^{-10}$
18	1.8×10^{-11}	9.9×10^{-10}	6.5×10^{-11}	$<5 \times 10^{-9}$
28	6.0×10^{-10}	8.0×10^{-10}	1.1×10^{-9}	$<1 \times 10^{-9}$
44	8.5×10^{-12}	2.1×10^{-10}	3.0×10^{-11}	$<2 \times 10^{-9}$
all other AMUs	7.7×10^{-11}	7.4×10^{-10}	1.1×10^{-10}	$<1.9 \times 10^{-9}$

bakeout. The sensor suite includes current and voltage monitors, thermocouples, pressure gauges, simple strain monitoring setups, residual gas analysis systems (RGAs), 8 cryopumps and turbomolecular pumps.

The data acquisition system generates ~ 400MB of data per bakeout (~3 GB for both observatories). Data are ingested into a database at Caltech which is then available via a web browser interface.

Table 2 shows the residual gases by species after the first bakeout (of four total) at LHO. Note that other than H₂ all other gases register as upper limits. The results meet LIGO requirements. No evidence of air leaks have been found to date for the more than ~90 km of welds required to fabricate the beam tubes.

Presently activities at LHO are focused on the installation of the first interferometer (2km). These will be discussed below, under interferometers. At LLO activities are just now starting on the single 4km instrument.

Table 2 Y1 Hanford [$Q < 1 \times 10^{-10}$ t-l/s]

Species	J @ 25C t-l/cm ² /s	p[mid-tube] 23C, end pump only
H ₂	6.3×10^{-14}	3.6×10^{-8}
H ₂ O	$< 2 \times 10^{-17}$	$< 1.4 \times 10^{-12}$
N ₂	$< 3 \times 10^{-19}$ [8C]	$< 5 \times 10^{-14}$ [8C]
CO ₂	$< 1.8 \times 10^{-18}$	$< 1 \times 10^{-12}$
H _n C _p O _q	$< 8.5 \times 10^{-19}$	$< 5 \times 10^{-13}$

of 0.0053 m at LHO and 0.0040 m at LLO. **Table 3** and **Table 4** present the relevant geophysical parameters which described the interferometer arms at the two observatories.

The bakeout utilizes ohmic [DC] heating of 304L SS BT wall to temperatures ~170C for durations of up to 15 days (360 hrs at temperature). ~1500 - 2000 A of DC current are required to maintain the elevated wall temperature [the value depends on the ambient environmental conditions]. The beam tube is baked one 2km section (a module) at a time. Each site requires 4 bakeouts. During bakeout an array of ~ 600 sensors along the module are monitored to ensure trouble-free operation and to monitor progress of the

Figure 4



A detailed in-house analysis of the GPS data on beam tube alignment for both sites was completed. The results of this analysis are presented in **Table 3** and **Table 4**. In summary, at each site the interferometer arms are aligned to an orthogonal coordinate system to an accuracy better than $\sim 1.3 \times 10^{-6}$ radians at LHO and $\sim 6.1 \times 10^{-6}$ radian at LLO.

The best fit axes give a residual 3-axis RMS

Table 3 Parameters resulting from best fit to the survey data for Hanford, WA

Parameter	Value	Estimated Error	Units
Vertex	Global $\{\hat{x}_G, \hat{y}_G, \hat{z}_G\}: \{0,0,0\}$	{0.0064,0.0073,0.0050}	m
	Geodetic $\{h, \phi, \lambda\}: \{142.554, \{46,27,18.528\}, \{-119,24,27.5657\}\}$	-	{m,deg, deg}
	Earth-fixed $\{\hat{x}_E, \hat{y}_E, \hat{z}_E\}: \{-2.1614149 \cdot 10^6, -3.8346952 \cdot 10^6, 4.6003502 \cdot 10^6\}$	{0.0066, 0.0057, 0.0054}	m
\hat{x}_G axis	Global $\{\hat{x}_G, \hat{y}_G, \hat{z}_G\}: \{1,0,0\}$	-	
	Earth-fixed $\{\hat{x}_E, \hat{y}_E, \hat{z}_E\}: \{-0.223892, 0.799831, 0.556905\}$	-	
	Compass Direction: N35.9994° W (ref. geodetic north) ^a	$1.93 \cdot 10^{-6}$	radian
	Angle relative to local horizontal at Vertex: $-6.195 \cdot 10^{-4}$	$2.73 \cdot 10^{-6}$	radian
\hat{y}_G axis	Global $\{\hat{x}_G, \hat{y}_G, \hat{z}_G\}: \{0,1,0\}$		
	Earth-fixed $\{\hat{x}_E, \hat{y}_E, \hat{z}_E\}: \{-0.913978, 0.0260945, -0.404923\}$		
	Compass Direction: S54.0006° W (see footnote a)	$1.93 \cdot 10^{-6}$	radian
	Angle relative to local horizontal at Vertex: $-1.25 \cdot 10^{-5}$	$2.73 \cdot 10^{-6}$	radian
\hat{z}_G axis	Global $\{\hat{x}_G, \hat{y}_G, \hat{z}_G\}: \{0,0,1\}$		
	Earth-fixed $\{\hat{x}_E, \hat{y}_E, \hat{z}_E\}: \{-0.338402, -0.599658, 0.725186\}$		
	Deviation from zenith at vertex: $6.195 \cdot 10^{-4}$, toward \hat{x}_G	$2.73 \cdot 10^{-6}$	radian

a. Site drawings call for arms to run N36.8° W and S53.2° W; these are referred to the WA state plane coordinates (northing & easting). Geodetic north is 47°39' (~0.8°) W of grid north at the vertex.

Table 4 Parameters resulting from best fit to the survey data for Livingston, LA

Parameter	Value	Estimated Error	Units
Vertex	Global $\{\hat{x}_G, \hat{y}_G, \hat{z}_G\}: \{0,0,0\}$	{.0062, .0055, .0041}	m
	Geodetic $\{h, \phi, \lambda\}: \{-6.574, \{30,33,46.4196\}, \{-90,46,27.2654\}\}$	-	{m, deg, deg}
	Earth-fixed $\{\hat{x}_E, \hat{y}_E, \hat{z}_E\}: \{-74276.044, -5.496283721 \cdot 10^6, 3.224257018 \cdot 10^6\}$	{.0062, .0055, .0041}	m
\hat{x}_G axis	Global $\{\hat{x}_G, \hat{y}_G, \hat{z}_G\}: \{1,0,0\}$	-	
	Earth-fixed $\{\hat{x}_E, \hat{y}_E, \hat{z}_E\}: \{-0.954574, -0.14158, -0.262189\}$	-	
	Compass Direction: S72.2835° W (ref. geodetic north) ^a	$1.73 \cdot 10^{-6}$	radian
	Angle relative to local horizontal at Vertex: $-3.121 \cdot 10^{-4}$	$2.44 \cdot 10^{-6}$	radian
\hat{y}_G axis	Global $\{\hat{x}_G, \hat{y}_G, \hat{z}_G\}: \{0,1,0\}$	-	
	Earth-fixed $\{\hat{x}_E, \hat{y}_E, \hat{z}_E\}: \{0.297741, -0.48791, -0.820545\}$	-	
	Compass Direction: S17.7165° E (see footnote a)	$1.73 \cdot 10^{-6}$	radian
	Angle relative to local horizontal at Vertex: $-6.107 \cdot 10^{-4}$	$2.44 \cdot 10^{-6}$	radian

Table 4 Parameters resulting from best fit to the survey data for Livingston, LA

Parameter	Value	Estimated Error	Units
\hat{z}_G axis	Global $\{\hat{x}_G, \hat{y}_G, \hat{z}_G\}: \{0,0,1\}$	-	
	Earth-fixed $\{\hat{x}_E, \hat{y}_E, \hat{z}_E\}: \{-0.0117515, -0.861335, 0.507901\}$	-	
	Deviation from zenith at vertex, toward \hat{x}_G : $3.121 \cdot 10^{-4}$ toward \hat{y}_G : $6.107 \cdot 10^{-4}$	$2.44 \cdot 10^{-6}$	radian

- a. Site drawings call for arms to run S72° W and S18° E; these are referred to the LA state plane coordinates (northing & easting). Geodetic north is 17' 1" (~ 0.28°) W of grid north at the vertex.

2 Interferometers

Seismic Isolation System [SEI]. Design of the system has been completed and first article testing was complete with the exception of the servo control design for the fine actuation of the (large) stacks. **Figure 7** shows one of the transfer functions measured for the HAM SEI stack during first article testing. The fine actuator subsystem design meets its requirements and all components are either in production or procurement at this writing. Production is well advanced and all procurement risks and virtually all fabrication and installation risks have passed. **Figure 5** shows the ~3m tall support piers for the BSC SEI.

To date 8 of 12 of HAM in-vacuum components have been accepted and 3 of 15 of in-vacuum components for BSCs. Completion is scheduled for September 1999.

Figure 5 BSC seismic isolation system support piers, LHO



The HAM assembly is shown in **Figure 6**.

Figure 6 HAM in-vacuum components, LHO



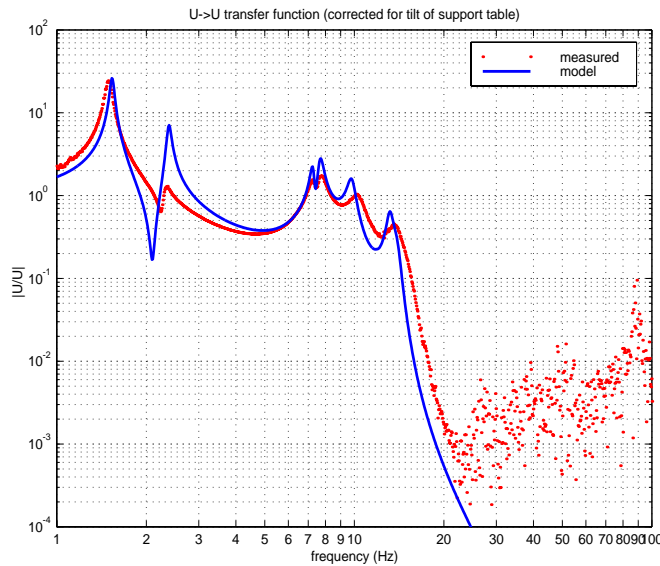
In-vacuum components are isolated from the external parts by flexible large-aperture bellows. To date 14 of 14 HAM bellows and 13 of 16 of BSC bellows have been delivered.

The interface between vertical piers and the horizontal support beams is a spherical air bearing assembly. To date 8 of 27 sets have been accepted.

Coarse adjustment of the integrated assemblies is performed using a coarse actuator subsystem which uses lead screw technology and stepper motors. To date 2 of 9 3-axis sets have been delivered and 0 of 6 vertical adjustment sets have been

accepted. The air bearing sits atop a rigid scissors table which is controlled by the coarse actuator. To date 8 of 12 HAM scissors tables and 3 of 15 BSC tables have been received.

Figure 7 Transfer function along beam axis



.SEI control electronics and racks are situated in the vicinity of each chamber to control the actuation systems. To date 1 of 4 racks has been delivered.

Suspension systems [SUS]. LIGO optics sit atop SEI subsystem assemblies in small and large versions of an optical suspension system [SOS and LOS respectively]. To date all design issues with LOS components have been resolved and 28 of 28 units have been received. This includes spacers [height adapters] needed to position identical LOS units at different heights in various chambers. At present units are being prepared for vacuum installation by cleaning and baking. **Figure 8** depicts an LOS with the 2km recycling mirror installed.

.The SOS assemblies (**Figure 9**) are used to suspend the smaller input optics for LIGO interferometers. Input optics subsystems [IO] are being delivered by University of Florida collaborators. To date all assemblies needed for the 2km interferometer have been fabricated, assembled and delivered. Most SOS assemblies needed for the LLO 4km instrument are presently complete and awaiting vacuum-preparation.

Figure 8 LOS assembly with recycling mirror being adjusted, LHO.



Figure 9 SOS assembly at LHO



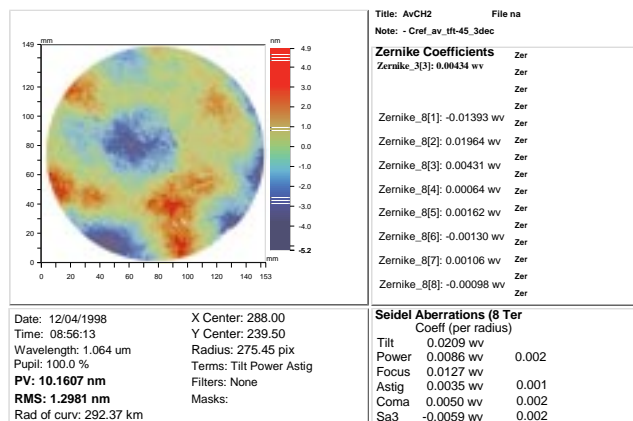
Both types of suspensions incorporate actuators and sensing to control suspended optics. These involve voice coil electromagnets which react against small strong dipolar magnets bonded to the mirrors. Local sensing is achieved using photodiode-photodetector pairs operating as edge sensors. To date sufficient quantities have been fabricated for the 2km interferometer. At mid-stage of the initial fabrication phase, problems with coil shorts and vacuum compatibility of photodiodes were identified. Coils developed shorts in the fabrication process and the photode-

tectors were discovered to come in two varieties, only one of which had been approved for use in LIGO. All units had to be reworked to resolve the electrical shorting problems and vacuum compatibility testing is presently under way to resolve the potential contamination problem.

In the course of assembling 2km suspended optics, it was discovered that there were procedural issues associated with how the minute, powerful dipole magnets were bonded to the pristine mirror surfaces and sides. In an unacceptable number of instances, the magnet assemblies were found to break off unexpectedly. A “tiger team” is presently investigating the problem. Tentative solutions which have been identified include curing of the bonding epoxy at more elevated temperatures, omitting a wet bath soak step which was included to clean the optical surfaces just before installation, and identifying different bonding techniques, such as adoption of the indium bump bonding technique which is common in the semiconductor industry.

In addition, a slight modification was introduced to control electrostatic build up on certain range-limiting mechanical stops which are needed to limit optics swing. This involved using minute fluor-rel-tipped Ag-coated SS screws.

Figure 10 Large optic phase map measured at Caltech



Final metrology on all as-built optics is being performed at Caltech. For this purpose, LIGO had a large-aperture interferometer modified by the vendor to operate at 1064 nm. **Figure 10** shows a phase map measured at Caltech. Measurements have been shown to be reproducible to 1 nm RMS for surface roughness (high spatial frequency errors) and 2% in absolute radius-of-curvature [ROC] measurements. Data indicate that polished-plus-coated optics are smooth to better than 1 nm RMS. In addition the ROC measurements are also within specified limits.

For measuring surface figure at the very highest spatial frequencies, it is possible to deduce surface figure errors from the amount of scattering produced [i.e., the bi-reflection distribution function, BRDF]. To measure scatter, LIGO had designed and built a special instrument [RTS monitor, for reflection, transmission and scatter].

An in-situ cleaning procedure will be needed and the method of choice which has been developed is the use of CO₂ snow blown across and optic to remove

Core optics components [COC]. To date all LIGO optics except for 3 input test masses [ITMs] and 3 recycling mirrors [RMs] have been delivered by CSIRO from Canberra, Australia. With the exception of 6 ITMs, 4 end test masses [ETMs] and 3 RMs, all other optics have been successfully coated with high reflectance [HR] coatings required by LIGO.

Figure 11 shows a polished and coated LIGO beamsplitter.

Figure 11 LIGO beamsplitter

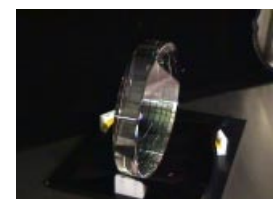
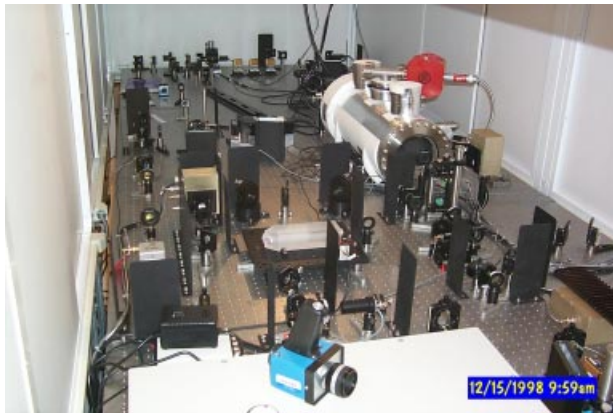


Figure 12 2km PSL assembly at LHO



Prestabilized laser system [PSL]. LIGO has accepted delivery of all (5) 10W lasers from the vendor, Lightwave Electronics [LWE]. These units meet all power, beam quality, frequency and amplitude noise specifications. Initial reliability problems with pump diodes (i.e., power output degradation over time) appear to have been successfully resolved by LWE through its quality assurance program [QA]. An improved design for the master oscillator which promises to provide better frequency and amplitude noise performance is being pursued with LWE in anticipation of higher output light sources needed for LIGO II enhancements.

At Hanford, the laser for the 2km interferometer has been integrated by LIGO into a prestabilized laser subsystem. Performance testing is nearly complete and results are under analysis. Further PSL characterization will have to await availability of the LIGO 12m suspended mode cleaner to provide better diagnostics. All servo loops (5 total for the PSL) are functioning, although some minor adjustments of loop parameters are indicated to improve in-loop noise performances. A diagnostics test suite is being implemented in software to exercise the PSL more fully.

LLO PSL installation for the 4km interferometer began April 1999. **Figure 13** shows the intensity noise performance of the 2km PSL subsystem. Further details on LIGO's PSL appear elsewhere in these proceedings [B. Wilke et al.].

Input optics [IO]. The input optics subsystem was designed, specified, fabricated and will be installed by the University of Florida group [UFI]. To date all optics for the three IO systems have been polished and coated. IO installation on the 2km interferometer at LHO is proceeding. The in-air optics bench and all optics have been installed and aligned. Most of the SOS in-vacuum units have been installed, although the magnet stand-off breakage issue is causing some minor delays. The mode-matching telescope, the first subsystem to employ full-aperture optics, was installed. The 12m mode cleaner is being installed and shakedown tests are expected in May 1999. **Figure 14** shows a schematic of the IO. **Figure 9** above shows UFI researchers at Hanford performing SOS installation of IO components.

Figure 13 Relative intensity noise for the servo-controlled PSL, LHO.

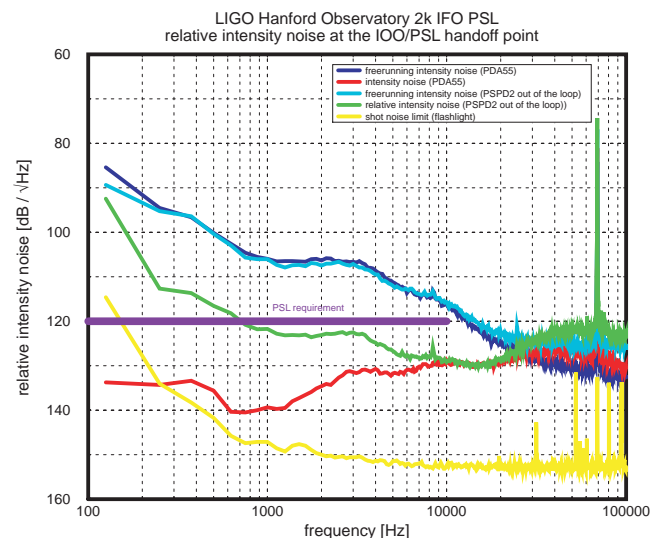
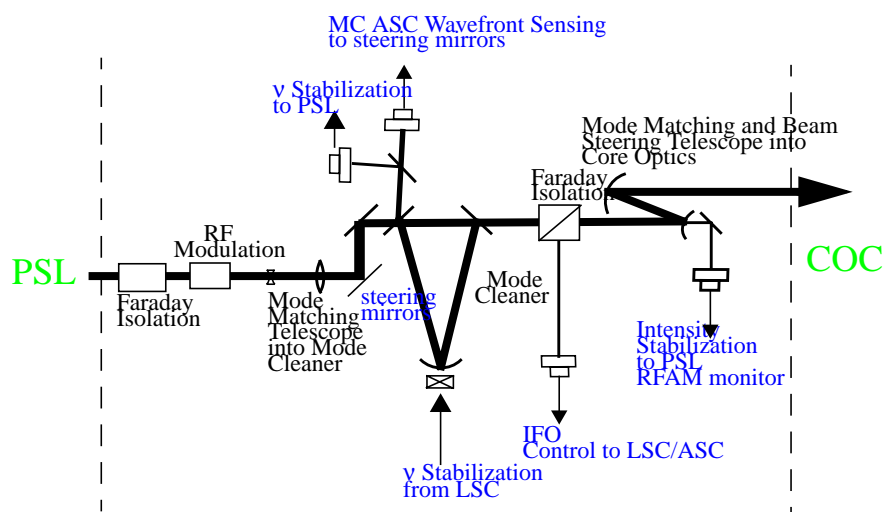


Figure 14 Layout of the IO subsystem.



A mode-matching wavefront sensing experiment is proceeding at UFL. This annular wavefront sensor is used to maintain focus of the input telescope into the interferometer recycling cavity. The first working unit for the 2km interferometer is scheduled for delivery at Hanford in June 1999.

Preliminary alignment of the in-vacuum IO components has been performed with an attenuated PSL beam.

At Livingston, Louisiana, IO installation will begin May 1999.

Interferometer Sensing and Control [ISC]. The ISC subsystem is responsible for the servo-control of the suspended optics to maintain operational performance of the LIGO interferometers. This subsystem is divided into Alignment Sensing and Control [ASC] and Length Sensing and Control [LSC]. The initial rough alignment of the interferometers as they are built up is also the responsibility of this group. At present activities are focused on setting up at LHO for the 2km instrument.

All optical-quality viewports for the 2km interferometer have been installed and vacuum checked. Viewports for LLO are scheduled for April 1999 delivery.

In October 1998 a dummy end test mass was aligned. In December 1998 a successful simulated test of lock acquisition was demonstrated. **Figure 15** shows a test set up at MIT.

Figure 15 ASC/LSC bench tests at MIT



One significant milestone achieved on the 2km interferometer in January 1999 was the successful transmission of an alignment beam through the 2km beam tube. The dead-reckoning alignment was within ~5cm of the desired position. This milestone also confirmed the GPS alignment of the beam tubes during their fabrication.

The first of the in-air optics benches dedicated to ASC/LSC were delivered to LHO in January 1999. In-air, in-situ alignment of large optics was successfully performed in February 1999. Also in February a successful end-to-end integrated test of the digital signal processors [DSPs] for servo and supervisory control was achieved.

The ASC/ISC will be first used to bring the IO subsystem under alignment and control during its commissioning in May 1999.

Control & Data Systems [CDS]. CDS is responsible for the real-time data and control functions for interferometer operations. All major subsystems described above are comprised of significant CDS components in addition to their mechanical or electro-optical components.

The electronics and servo controls for the 2km PSL are completed and have been commissioned. The 4km PSL at LLO is in process of being installed by the same team.

Suspension system controls have been installed and tested for the 2km IO subsystem. The LLO counterparts are in process of being installed. All vertex Michelson interferometer large optics [LOS] controls have been installed and tested for the 2km interferometer. At LLO a suspension test stand used for preliminary testing and calibration is being set up.

ASC/LSC controls are presently being installed at LHO for supporting commissioning of the 2km IO subsystem. Designs are complete for wavefront sensing components, and production for the 2km interferometer has begun. The LSC dark port photodiode assembly design is complete and the 2km first article was expected in April 1999. Prototype control algorithm and software are being developed for servo loops.

The Data Acquisition System [DAQS] is being implemented at both observatories. The networking infrastructure along the 4km arms has been put in place. Servers have been set up and the first release of acquisition software is operational at both sites. This includes the ability to acquire data in LIOG/VIRGO frame format; viewing data subsets in real-time; data distribution over the site LAN; data extraction from frames.

3 Data Analysis and Simulations

LIGO Data Analysis System [LDAS]. The data analysis system for LIGO successfully completed a preliminary design in March 1999. Further details of the data analysis system appear later in these proceedings and will not be presented here [J.K. Blackburn et al.]. Software development began in earnest after the detailed design was completed. LDAS will be released in a 4-stage development effort which will allow experience from users to be incorporated into design improvements over the next 3 years.

Initial release of $\alpha 1$ version software is planned for June 1999 and will focus on supporting commissioning of the IO + PSL subsystems on the 2km interferometer at LHO. This release will include data distribution and limited archiving capacity at the site; limited data conditioning (numerical filtering) of raw data streams; metadata (data about data) archiving and querying. It will be targeted to a limited user base to determine what works and what is needed, No parallelized computational analysis of interferometer data will be supported at this phase.

An update release, $\alpha 2$ is planned for October 1999. This release will include the ability to run MPI-based parallelized computational analysis of interferometer data.

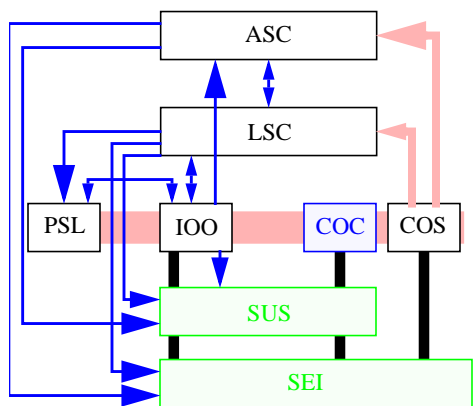
A full β release is planned for December 2000. This will include a full complement of user interfaces allowing researchers to access LIGO data with web tools and over the internet (at limited bandwidth, of course). The β release will also enable scientists to access archived data stored at LIGO's Caltech archive housed at the Center for Advanced Computing Research [CACR].

The first official Version 1 release is presently planned for January 2002 and will be concurrent with the planned LIGO I science run. At this time full availability of all data analysis resources (please refer to paper by J.K. Blackburn et al. in these proceedings for further details) will be included.

Concurrent with each of the various stages of software release, LIGO Laboratory and the Scientific Collaboration will performed certain "mock data challenges" to ensure the integrity of the software

framework and hardware systems.

Figure 16 Organizational schematic of the E2E environment



LIGO Simulation: the End-to-End Model [E2E]. Over the past two years LIGO has been developing a time-domain simulation environment which is optimized for simulating the optical and mechanical behavior of interferometers composed of Fabry-Perot cavities and suspended mirrors. The simulation environment is fully written in an object oriented paradigm using C++: there is a one to one mapping between software modules and physical hardware subsystems. The E2E framework includes modular “widgets” such as lasers, mirrors, digital filters, suspensions, seismic stacks, etc. The electromagnetic fields are projected in terms of cavity modes, so that higher order resonant behavior of misaligned cavities can be simulated. **Figure 16** depicts a schematic of the mapping of software onto hardware components.

The E2E simulation environment has been successfully ported and installed at a variety of LIGO sites and collaborating home institutions.

Examples of simulation capabilities presently available include: (i) projection of thermal displacement noise from mirrors and suspensions for LIGO I; (ii) the ability to fully model the 40m interferometer prototype (on the Caltech campus); (iii) simulation of highly non-linear cavity lock acquisition processes in the time domain; (iv) the ability to begin modeling novel future interferometer topologies in support of advanced R&D for LIGO II, etc. **Figure 17** presents a screen shot of a model built up within the E2E framework.

The development of ‘widgets’ within the E2E environment has become a collaborative enterprise including Caltech, MIT, UFl, Penn State and the University of Pisa. Internationally, collaboration to develop interferometer modeling tools includes VIRGO, GEO and TAMA.

4 Summary

In conclusion LIGO Project is within budget and foreseen to be able to begin scientific operations approximately on the same schedule developed in 1994. **Table 5** presents the key LIGO installation milestones.

Figure 17 Screen shot of a simulated model in the E2E environment

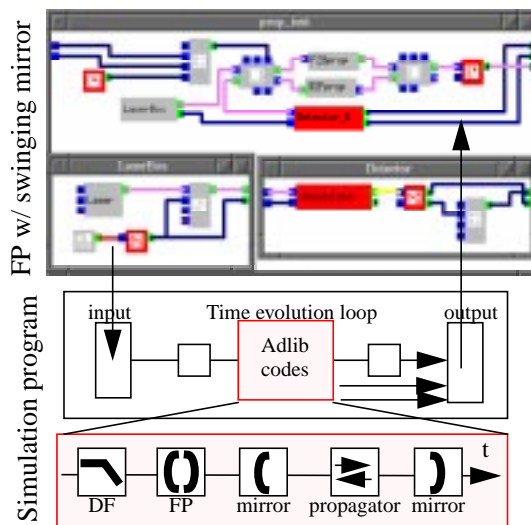


Table 5 LIGO Installation Major Milestones

Milestone	Date
Vacuum Equipment Complete	December 1998
BT Bakeout Complete	February 2000
LHO 2km Start	July 1998
Power Recycled	March 2000
Vertex Michelson complete	
LHO 2km IFO complete, $h[f] < 10^{-20}$	November 2000
LLO 4km Start	January 1999
Power Recycled	May 2000
Vertex Michelson complete	
LLO 4km IFO complete, $h[f] < 10^{-20}$	February 2001
LHO 4km Start	July 1998
Power Recycled	July 2000
Vertex Michelson complete	
LHO 4km IFO complete, $h[f] < 10^{-20}$	February 2001
Design sensitivity, $h[f] < 10^{-21}$	January 2002
First science run, 3X operation	February 2002

5 Acknowledgements

The work reported herein represents the collective efforts of the LIGO team who have been working to make LIGO become a reality. Without their tremendous spirit and dedication, I would have had little to report. I am indebted to all of them for the materials provided for this contribution.

The LIGO Project and LIGO Laboratory are supported by the National Science Foundation under cooperative agreement PHY-9210038.